

Artigo de Pesquisa

Suspended sediment transport estimation in Negro River (Amazon Basin) using MSI/Sentinel-2 data

O Transporte de sedimento suspenso no Rio Negro (Bacia Amazônica) por meio de dados MSI/Sentinel-2

Rogério Ribeiro Marinho ¹, Naziano Pantoja Filizola Junior ², Jean-Michel Martinez ³ e Tristan Harmel ⁴

¹ Universidade Federal do Amazonas, Departamento de Geografia, Manaus, Brazil. rogeo@ufam.edu.br

ORCID: <https://orcid.org/0000-0001-5219-8635>

² Universidade Federal do Amazonas, Departamento de Geociências, Manaus, Brazil. nazianofilizola@ufam.edu.br

ORCID: <https://orcid.org/0000-0001-7285-7220>

³ Institut de Recherche pour le Développement, Géosciences Environnement Toulouse, Toulouse, France. martinez@ird.fr

ORCID: <https://orcid.org/0000-0003-3281-8512>

⁴ Centre national de la Recherche Scientifique, Géosciences Environnement Toulouse, Toulouse, France.

tristan.harmel@get.omp.eu

ORCID: <https://orcid.org/0000-0002-1172-9636>

Recebido: 12/01/2021; Aceito: 07/05/2021; Publicado: 15/01/2022

Abstract: The dynamics of suspended sediment production and transport in large rivers are essential geomorphological processes that can influence biodiversity. The aim of this work was to analyze the spatio-temporal variation of suspended sediment transport in the lower Negro River using Sentinel-2 images. The suspended sediment concentration (SSC) was estimated from the reflectance of band 4 of the MSI sensor onboard the Sentinel-2A and Sentinel-2B. The results indicate that the hydrological regime controls the temporal variability of SSC, being higher in the low water period and lower during flooding, with a mean concentration of 5.28 mg L⁻¹ for the period 2015–2019. Analysis of the spatial variation of SSC in Sentinel-2 images indicated a zone of active sediment deposition located downstream of the islands of the Anavilhanas Archipelago. Geology, forest cover, and hydrological variability are the main factors controlling the low sediment yield of the basin, with an estimated suspended solid flux of 5.76×10⁶ ton·year⁻¹ and a specific yield of 8 ton·km⁻²·year⁻¹. Despite the lower quantity of images between February and April, due to high cloud cover, this study showed that Sentinel-2 images could be used to monitor the temporal and spatial dynamics of suspended sediment transport in Amazonian blackwater rivers.

Keywords: Suspended sediment concentration; Guiana Shield; Remote sensing.

Resumo: A dinâmica de produção e transporte de sedimento suspenso em grandes rios é um importante indicador de processos geomorfológicos que influencia a biodiversidade. O objetivo deste artigo foi analisar a variação espaço-temporal do sedimento suspenso no baixo Rio Negro utilizando imagens Sentinel-2. A concentração de sedimento suspenso (CSS) foi estimada a partir da banda 4 do Sentinel-2A e Sentinel-2B. A variabilidade temporal da CSS é controlada pelo regime hidrológico, maior no período de águas baixas e menor durante a inundação, com concentração média de 5,28 mg L⁻¹ para o período 2015-2019. Análise da variação espacial da CSS nas imagens Sentinel-2 indicaram uma zona de deposição ativa de sedimento situada à jusante das ilhas do Arquipélago de Anavilhanas. A geologia, a cobertura florestal e a variabilidade hidrológica são os principais fatores que controlam a baixa produção de sedimento da bacia, com um fluxo sólido suspenso estimado em 5,76×10⁶ ton·ano⁻¹ e produção específica de 8 ton·km⁻²·ano⁻¹. Apesar da menor quantidade de imagens entre os meses de Fevereiro e Abril, devido à elevada cobertura de nuvens, este estudo mostrou que imagens Sentinel-2 podem ser

utilizadas para monitorar a dinâmica temporal e espacial do transporte de sedimento suspenso em rios amazônicos com águas pretas.

Palavras-chave: Concentração de sedimento suspenso; Escudo das Guianas; Sensoriamento remoto.

1. Introduction

The transformation of the landscape and maintenance of the climate at different scales are strongly related to the action of surface water resources. Large rivers are considered the primary agents of transfer of erosion products to the oceans through sediment transport (GUPTA, 2007; MILLIMAN and FARNSWORTH, 2011). Therefore, monitoring the variability of sediment flux in different river systems contributes to the understanding of landscape formation, quantifying biogeochemical processes, and evaluating impacts of environmental changes of natural or anthropic origin (CHARLTON, 2007; FILIZOLA et al., 2011; TUCCI, 2012).

Among the ten largest rivers in the world in terms of water volume, four are located in the Amazon Basin (LATRUBESSE, 2008). The Negro River is the principal tributary of the left margin of the Amazon River. With an average annual water discharge of $28,400 \text{ m}^3\cdot\text{s}^{-1}$, this large river presents a complex multi-channel system, and its drainage basin has one of the lowest erosion rates in the Amazon (FILIZOLA and GUYOT, 2011; WITTMANN et al., 2011). However, the National Hydrometeorological Network does not carry systematic and regular measurements of sediment transport along more than 600 km of its lower course, mainly because of the presence of large river archipelagos and the low suspended sediment load (FILIZOLA and GUYOT, 2009).

The current environmental scenario in the Amazon presents challenges related to the conservation and management of natural resources; thus, integrating consolidated field techniques with the use of remote sensing data enables a better understanding of processes and factors related to the transport of suspended sediment by rivers in the region. However, estimating water quality in function of remote sensing reflectance data is still a major research challenge, considering the complexity of the optical properties of different river systems (MARTINEZ et al., 2015).

The Negro basin extends over part of Brazil, Colombia, Guyana, and Venezuela, with its upper part located on the Guiana Shield. This shield is composed of crystalline rocks of the Precambrian, with low and eroded relief (FILIZOLA and GUYOT, 2009). The tributaries of the Amazon River that drain the Guiana Shield present a low suspended load, with estimated values of $0.4 \text{ ton}\cdot\text{ano}^{-1}$ in the Jari River, $03 \text{ ton}\cdot\text{ano}^{-1}$ in the Trombetas River, and $08 \text{ ton}\cdot\text{ano}^{-1}$ in the Negro River (FILIZOLA, 1999). The Caura River, one of the principal tributaries of the Orinoco River that drains the Guiana Shield, also has black waters and a low concentration of suspended sediment (MORA et al., 2014).

The Negro River basin has the lowest density of sedimentometric stations among the large rivers of the Amazon basin (MARINHO; FILIZOLA; CREMON, 2020). The closest station to its mouth with regular measurements of suspended sediment concentration, called Serrinha (Code 14420000), is located about 600 km upstream from Manaus. Thus, the main estimates of the suspended sediment flux of the Negro River were made based on the contributions of stations located within the basin, hundreds of kilometers from the mouth. Thus, there is an absence of data from the Brazilian network of sedimentometric stations in this basin, which does not allow for the precise quantification of the suspended sediment discharge contributed by the Negro River to the Amazon River.

The launch of the Landsat-8 satellite and the Sentinel-2 satellite constellation has opened up new possibilities for the use of orbital data for terrestrial monitoring (LI and ROY, 2017). In particular, the Sentinel-2 constellation (Sentinel-2A and Sentinel-2B satellites) enables, since 2017, the acquisition of images with five-day review time, meaning an increased possibility of cloud-free images with higher spatial resolution than that of the images of the MODIS sensors (Terra and Aqua satellites) and the OLCI (Sentinel-3A and Sentinel-3B satellites), commonly used for the study of watercolor in coastal and ocean environments.

In this context, the aim of this work was to analyze the spatial-temporal variation of suspended sediment concentration in the lower Negro River using images from the Sentinel-2 satellite constellation. Thus, based on a dataset obtained between 2015 and 2019, this study presented seasonal estimates of the concentration and flux of suspended sediment in the Negro River near its mouth.

2. Study Area

The study was developed in the Tatu-Paricatuba hydrometric section (Latitude -3.081; Longitude -60.233), situated 17 km upstream of Manaus city and 45 km from the confluence of Negro and Solimões rivers (Figure 1). The drainage area of the Negro River in this section is 712,000 km². The mean width of the section is 2450 m, and the maximum depth of the talweg is above 60 m during the flood period (Figure 1c). The Negro River in this section presents a slight vertical variation of suspended sediment transport as a function of depth (MARINHO; FILIZOLA; CREMON, 2020), where the flow of sediment transported in suspension corresponds to 80% of the total flow of the section (FILIZOLA, 2003).

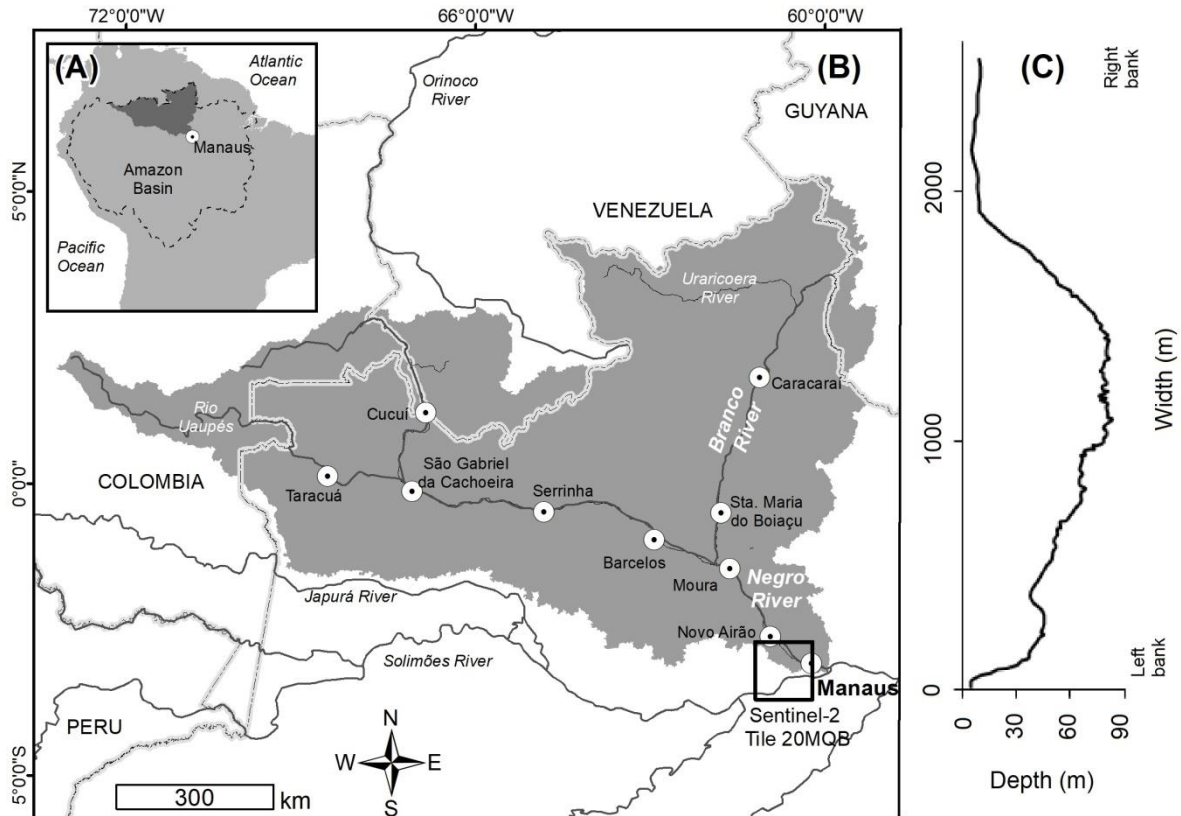


Figure 1. Location of the study area. (a) Amazon Basin; (b) Negro Basin and the Tatu-Paricatuba hydrometric section (black polygon); (c) Cross-sectional profile of the Tatu-Paricatuba hydrometric station in July 2017.

According to Koppen's climatic classification, the region has a tropical climate without a dry season (type Af). The average annual precipitation in the basin is of the order of 2000 mm. The average annual water discharge is estimated at 28,400 m³·s⁻¹ (MOLINIER et al., 1996) with a hydrological regime characterized by a rising period between December and May, a flood peak in June-July, falling in August and September, and low water in October and November. In general, the annual hydrological regime presents a normal behavior, with average variability of the level, between flood peak and low water, of the order of 10 m in Manaus. It is noteworthy that the variability of the height of the levels of the lower course of the Negro River is controlled by the hydraulic backwater caused by the Amazon River, which extends for more than 300 km upstream of its mouth (MEADE et al., 1991).

The Negro River drains ancient and tectonically stable terrains of the Guiana Shield, with a suspended sediment production of less than 10 ton·km⁻²·year⁻¹ (FILIZOLA and GUYOT, 2009). Approximately 50% of this sediment production comes from the Branco River, the largest tributary of the basin and the main river of the state of Roraima (SANDER et al., 2014). The water of the Negro River has a dark color due to the high concentration of dissolved organic carbon, with an average of 8 mg L⁻¹ (LEENHEER, 1980; RICHEY et al., 1990), and the low concentration of suspended sediment, around 5 mg L⁻¹ (FILIZOLA and GUYOT, 2011; MARINHO; FILIZOLA; CREMON, 2020; MEADE et al., 1979).

2. Materials and Methods

2.1. Estimation of suspended sediment concentration

The concentration of suspended sediment (SSC) transported by the Negro River was estimated based on water samples collected between 2016 and 2019 in its lower course. A fixed area of the river section was used to collect surface water samples in nine georeferenced points (Figure 2) proposed by Filizola et al. (2009). The laboratory procedures to determine SSC followed the protocol of Hybam (2018), which consists of filtering water samples in cellulose acetate membranes (porosity of 0.45 μm). After filtration, the filtered sample was heated for two hours in an oven at 105 °C. The SSC was determined from the difference between the initial and final weights of the filtered sample divided by the sample volume. Simultaneously with the collection of surface water samples, remote sensing reflectance (Rrs) hyperspectral measurements were performed to adjust empirical models that relate the SSC as a function of Rrs measured considering the spectral characteristics of the multi-spectral instrument (MSI) sensor onboard the Sentinel-2A and Sentinel-2B satellites.

Suspended inorganic sediment has a higher scattering coefficient than that of organic particulates owing to its higher refractive index (BUKATA, 2005; DOXARAN et al., 2002). In general, the higher the SSC, the more significant the magnitude of the reflectance until a saturation plateau. As a trade-off between reflectance increase and saturation phenomenon, measurements in the longer wavelengths of the visible-near-infrared part of spectrum are the most suitable for sediment load estimation, mainly in the red (620-760 nm) and near-infrared (760-1200 nm) bands. Thus, this study used the empirical model developed by Marinho et al. (2021) that estimates the SSC of Negro River from the reflectance of the red band of the MSI sensor, as shown in Eq. (1).

$$SSC = 881,4 \times B4 + 2,3 \quad (1)$$

where SSC is the suspended sediment concentration (in mg L^{-1}), and B4 is the remote sensing reflectance (in sr^{-1}) of Negro River detected by Sentinel-2 MSI sensor in band 4 (Rrs at 665 nm). As highlighted earlier, the data used to build this model were collected between 2016 and 2019 in the lower Negro River and region of the confluence with Branco River, with SSC ranging from 0.44 to 22.64 mg L^{-1} . The fit of this model showed R^2 of 0.86, mean square error estimates of 2.20 mg L^{-1} , and mean absolute error of 25% (MARINHO et al., 2021).

2.2. Sentinel-2 MSI images

A set of images from the MSI sensor onboard the Sentinel-2A and Sentinel-2B satellites, acquired between 2015 and 2019, were used to monitor SSC's temporal and spatial dynamics in the Tatu-Paricatuba gauge station of the Negro River. The Sentinel-2 satellite constellation is a part of the Copernicus Earth observation program coordinated by the European Commission and the European Space Agency. The Sentinel-2A and Sentinel-2B satellites were launched in 2015 and 2017, respectively, and have as payload the MSI sensor, developed to monitor the natural resources of the Earth's surface in high resolution. The band 4 MSI image used in this study has a wavelength centered at 665 nm, with a bandwidth of 30 nm in the red spectral region and a spatial resolution of 10 m. The main spectral and spatial characteristics of the MSI sensor and the Sentinel-2 mission can be found in Drusch et al. (2012).

The Sentinel-2 images used in this study were processed for atmospheric correction and sunglint reduction (specular reflection of direct sunlight on the water surface) using the Glint Removal of Sentinel-2-like images (GRS) algorithm developed by Harmel et al. (2018). As per these authors, the GRS algorithm performs both atmospheric correction and sunglint removal of Sentinel-2 images with L1C processing level. Thus, after atmospheric correction and sunglint removal, the band 4 water surface Rrs values of Negro River were extracted for a set of 79 images from Sentinel-2A and Sentinel-2B satellites acquired between August 2015 and January 2019.

The extraction of Rrs values from Sentinel-2 images was performed using the Sentinel Application Platform software (SNAP Desktop v. 7.0). In each Sentinel-2 image, after removing outliers, the average Rrs value of the set of pixels over a 700 x 700 m area of the Negro River was extracted (Figure 2). Thus, the selected pixels' average Rrs was considered representative of the reflectance on the given day of the satellite pass. On average, 1150 pixels per image were analyzed, ranging from 450 to 1500 pixels. The criteria of Montanher et al. (2014) were used to avoid pixels over shallow water areas, with background effects, riverbanks, islands or clouds, sandbanks, aerosol plumes, and radiometric noise. To avoid some of these effects present in 19 images, the sampling of pixels was performed slightly upstream of the section (yellow polygon in Figure 2).

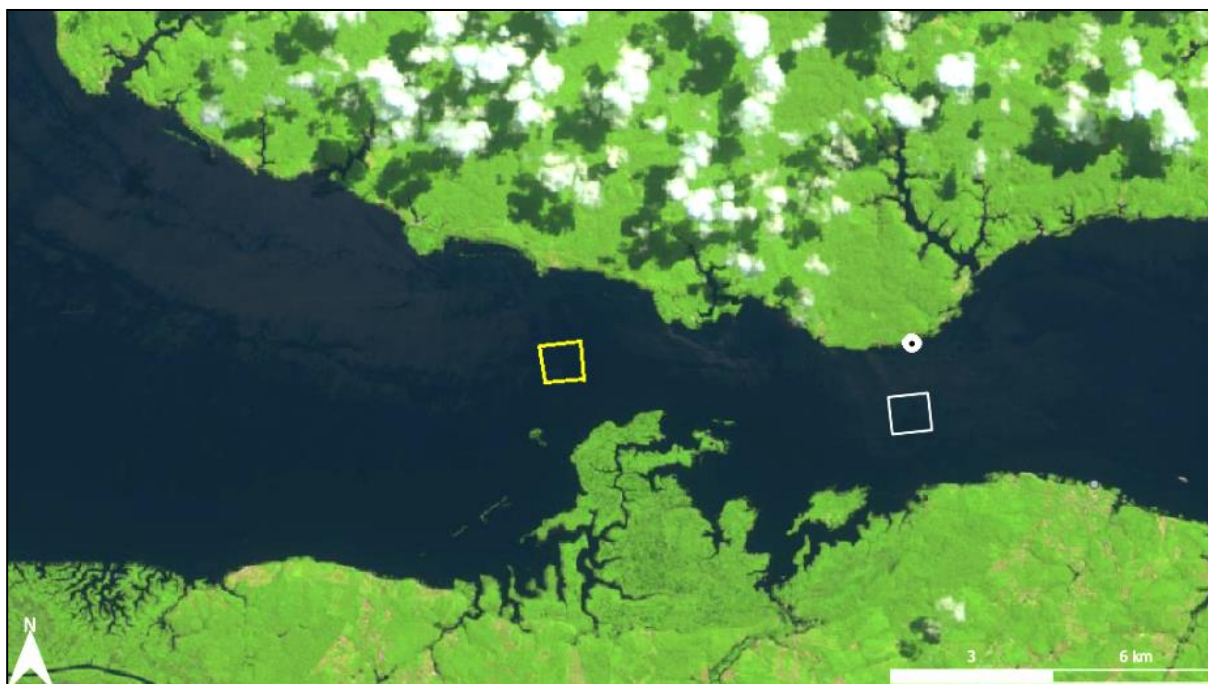


Figure 2. Example of pixel sampling in a Sentinel-2 image (false color composition). The pixel selection area is represented by the white polygon. The location of the Tatu-Paricatuba gauge station is indicated by the white dot.

2.3. Analysis

The seasonal and spatial variability of the SSC of the lower Negro River in the Tatu-Paricatuba gauge station was analyzed for the period 2015–2019 from Sentinel-2 satellite data. The variability of suspended sediment transport estimated by satellite was analyzed as a function of river regime and precipitation. For this, water level and discharge data from hydrometric stations located in the Negro and Branco rivers (Table 1) and precipitation data were used. The precipitation data used in this study are the monthly average values estimated for the Negro River basin by the CHIRPS v.2 product, which has 0.05 degrees of spatial resolution and offers spatialized estimates of precipitation at annual, monthly, and daily time intervals (CHIRPS, 2015). The use of this database is recommended for regions with a low density of rainfall stations. Evaluation by Costa et al. (2019) indicates that CHIRPS data are highly similar to rainfall station data.

Table 1. Conventional hydrometric stations analyzed. The location of these stations can be seen in Figure 1.

Code	Name	River
14790000	Santa Maria do Boiaçú	Branco
14990000	Manaus	Negro

Analysis of hydrosediment dynamics was performed based on data of water discharge, flow direction, and average flow velocity collected with an Acoustic Doppler Current Profiler (ADCP model Workhorse Rio Grande, Teledyne RDI) operating at a frequency of 600 kHz (MARINHO, 2019). The instantaneous suspended sediment discharge (Q_s), the mean annual sediment discharge (Q_{sa}), and the specific sediment yield (Q_{sp}) of the Negro River were obtained using the following Eq. (2), Eq. (3) and Eq. (4):

$$Q_s = Q \times SSC \times 0.0864 \tag{2}$$

$$Q_{sa} = Q_s \times 365 \tag{3}$$

$$Q_{sp} = Q_{sa}/Ab \tag{4}$$

where, Q is the water discharge of the section ($m^3 \cdot s^{-1}$); SSC is the suspended sediment concentration ($mg \cdot L^{-1}$); 0.0864 is a conversion factor used to transform the units into $ton \cdot day^{-1}$; Ab is the area of the Negro River basin ($712,000 \text{ km}^2$).

Relationships between SSC data estimated with Sentinel-2 and water level, water discharge, and precipitation data were assessed using scatter plots, the coefficient of determination (R^2), and Pearson's correlation coefficient (r). The normality of the SSC data was assessed using the Shapiro-Wilk test. Statistical tests were performed to evaluate the equality of means (t-test: $H_0: \mu_1 = \mu_2$) and variances (F-test: $H_0: \sigma_1 = \sigma_2$) of the estimated SSC near the right and left banks of the Negro River downstream of Anavilhanas Archipelago. The significance level adopted for the tests was 0.05 ($\alpha = 5\%$).

3. Results

3.1. Temporal variation of suspended sediment concentration

This study evaluated 79 Sentinel-2 images, and the mean SSC of the Negro River estimated for the period 2015–2019 was 5.28 mg L^{-1} , ranging from 1.96 mg L^{-1} to 15.11 mg L^{-1} . During the rising and falling periods, the SSC showed mean values of 5.53 mg L^{-1} ($n = 23$) and 5.08 mg L^{-1} ($n = 27$), respectively. Alternatively, during flood and low water periods, the Negro River presented mean values of 3.47 mg L^{-1} ($n = 19$) and 8.70 mg L^{-1} ($n = 10$), respectively. Figure 3 presents the time series of SSC estimated between August 2015 and January 2019.

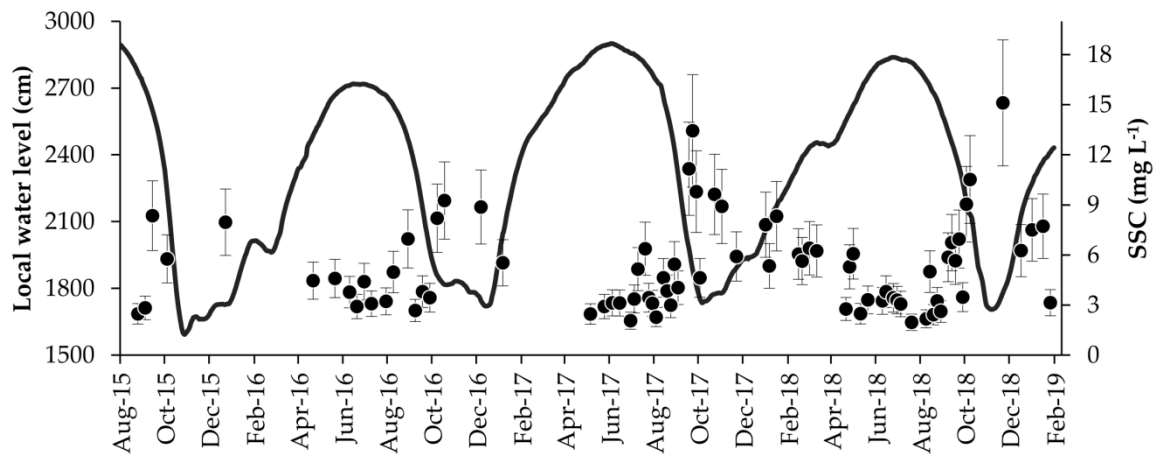


Figure 3. Time series of SSC from Sentinel-2 imagery (points) in the Tatu-Paricatara gauge station and the variability of the Negro River water level at Manaus (line). The bars in the points indicate the error of the SSC estimates.

The minimum and maximum values estimated in this dataset were observed in July and September 2018, respectively (Figure 3). Despite the short time series, we observed that the mean SSC values in the rising and falling are close (Table 2), but we noticed a greater amplitude and higher coefficient of variation of the data in the falling water period of the Negro River. We emphasize that there are no hydrometric stations with SSC measurement in the lower Negro River, a situation that makes it difficult to understand the temporal pattern of this study area based on a more extensive dataset.

Table 2. Descriptive statistics of SSC (in mg L^{-1}) estimated from Sentinel-2 data.

	Rising (Dec-May)	Flood (Jun-Jul)	Falling (Aug-Sep)	Low (Oct-Nov)
Images analyzed	23	19	27	10
Minimum	2.46	1.96	2.17	4.63
Maximum	8.87	6.37	13.44	15.11
Amplitude	6.41	4.41	11.27	10.48
Average	5.53	3.47	5.08	8.70
Median	5.63	3.25	4.04	8.98
25th percentile	3.31	3.08	2.83	5.87
75th percentile	7.50	3.77	6.74	9.85
Standard deviation	1.99	0.99	2.88	2.96
Coefficient of variation	36.01	28.62	56.62	34.06

Figure 4 presents the mean monthly variability of SSC obtained for this time series (2015–2019), where strong coefficients of determination and negative correlations were observed with the mean monthly variability of precipitation (Figure 4a with $R^2 = 0.74$ and $r = -0.79$) and river regime (Figure 4b with $R^2 = 0.92$ and $r = -0.96$). This variability indicates lower SSC in the rainy months, when the Negro River is in the rising and high water period. Contrastingly, when the precipitation period reduces, an increase of the mean monthly SSC was observed during the low water period.

A lag of five months was detected between the maximum concentration of suspended sediment (November) and the maximum level of the Negro River (June). As previously mentioned, the main tributary of water discharge and suspended sediment in the lower Negro River is the Branco River. With its mouth located more than 250 km from the study area, the Branco River has a different fluvial regime from the Negro River, with flood peak occurring at the beginning of the second half of the year, four months before the maximum SSC, besides having a flood pulse with a large amplitude of levels, in comparison to that of the Negro River at Manaus (Figure 4b). This lag can result from the joint action of the contributions coming from the Branco River and the influence of the backwater effect of the Amazon River, which controls the variability in the height of the levels of the lower Negro River.

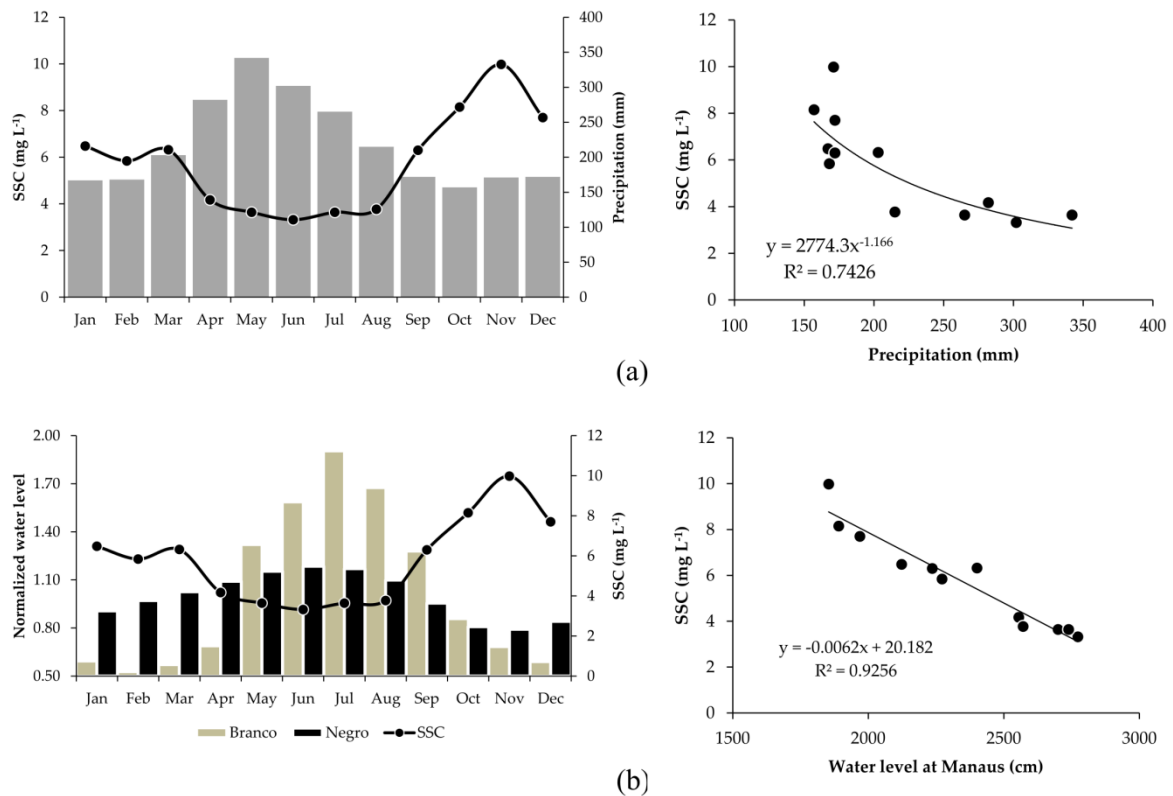


Figure 4. (a) Mean monthly variability of SSC (line) and precipitation (bar) and scatter plot; (b) Mean monthly variability of SSC (line) and mean monthly normalized water level in relation to the annual mean of Negro River in Manaus and Branco River (bars) and scatter plot between SSC and Negro River water level. Data period: 2015–2019.

The dynamics identified with Sentinel-2 data indicate that in the Negro River, an increase in mean SSC occurs at the end of the falling and during the low water period (September to December), which can be related to the greater volume of water contributed by the Branco River (Figure 4b). During the falling and low water periods, the precipitation in the region is lower (Figure 4a), and the Branco River starts to have a more significant influence on the fluvial dynamics of the study area. It is noteworthy that the mean SSC between September and December (8.03 mg L⁻¹) is twice as high as the mean SSC observed between April and August (3.71 mg L⁻¹). Thus, when the Negro River is at falling, the Branco River is still at the high water, a period in which there is a more outstanding contribution of suspended sediment in the study region.

3.2. Spatial variation of suspended sediment concentration

The spatiotemporal distribution of SSC in Negro River near the Tatu-Paricatuba hydrometric section was analyzed in images acquired in 2016, 2017, and 2018 in different hydrological periods (Figure 5, Figure 6, and Figure 7). This hydrometric section is located downstream of the Anavilhanas Archipelago, a complex multichannel reach of the Negro River. It presents a considerable reduction in the width of the Negro River channel, ranging from 12 km downstream of the last islands of the archipelago to about 2 km in the Paricatuba Strait.

In Figure 5, it is possible to verify the morphology of the Negro River channel in the Sentinel-2 images, with its fluvial valley blocked (LATRUBESSE and FRANZINELLI, 2005) and extensive areas of free water with a width greater than 10 km. This reach of Negro River presents a heterogeneous spatial and temporal distribution of suspended sediment, mainly during low water periods, with higher SSC near the left bank of the channel and decreased SSC towards the center of the channel.

During the Negro River flood, we noticed more uniformity in the spatial distribution of suspended sediment in this extensive open water area (Figure 5). The spatial dynamics of SSC in Negro River detected in Sentinel-2 images show that suspended sediments can vary seasonally and spatially depending on local morphology and sediment input from Branco River and according to the hydrological period.

In the Paricatuba Strait, due to the abrupt reduction of the channel width (funnel effect), the mean flow direction of the Negro River is 96° from North clockwise, which can contribute to the maintenance of suspended sediment in the areas near the left margin. The mean annual velocity of the river flow in this section is $0.4 \text{ m}\cdot\text{s}^{-1}$, with an annual variation of 0.3 to $0.5 \text{ m}\cdot\text{s}^{-1}$ in the rising and falling water periods, respectively. Owing to the hydraulic control of the Amazon River over the Negro River, the highest velocities are observed in the transition period from rising to falling (between June and September) but about three times lower than that of the Amazon River.

The statistical analysis results indicate that the mean and variance of SSC between the left and right banks are distinct (Figure 6a). In general, the mean SSC observed in the right bank channel (4.05 mg L^{-1} , $n = 66$) was 30% lower than the mean SSC in the left bank channel (5.75 mg L^{-1} , $n = 61$). The normality test indicates that the data set presents normal distribution (H_0 : the data has a population with normal distribution). In Figure 6b, we can observe the SSC variation along a cross-section of the Negro River between the high and low water periods of 2018.

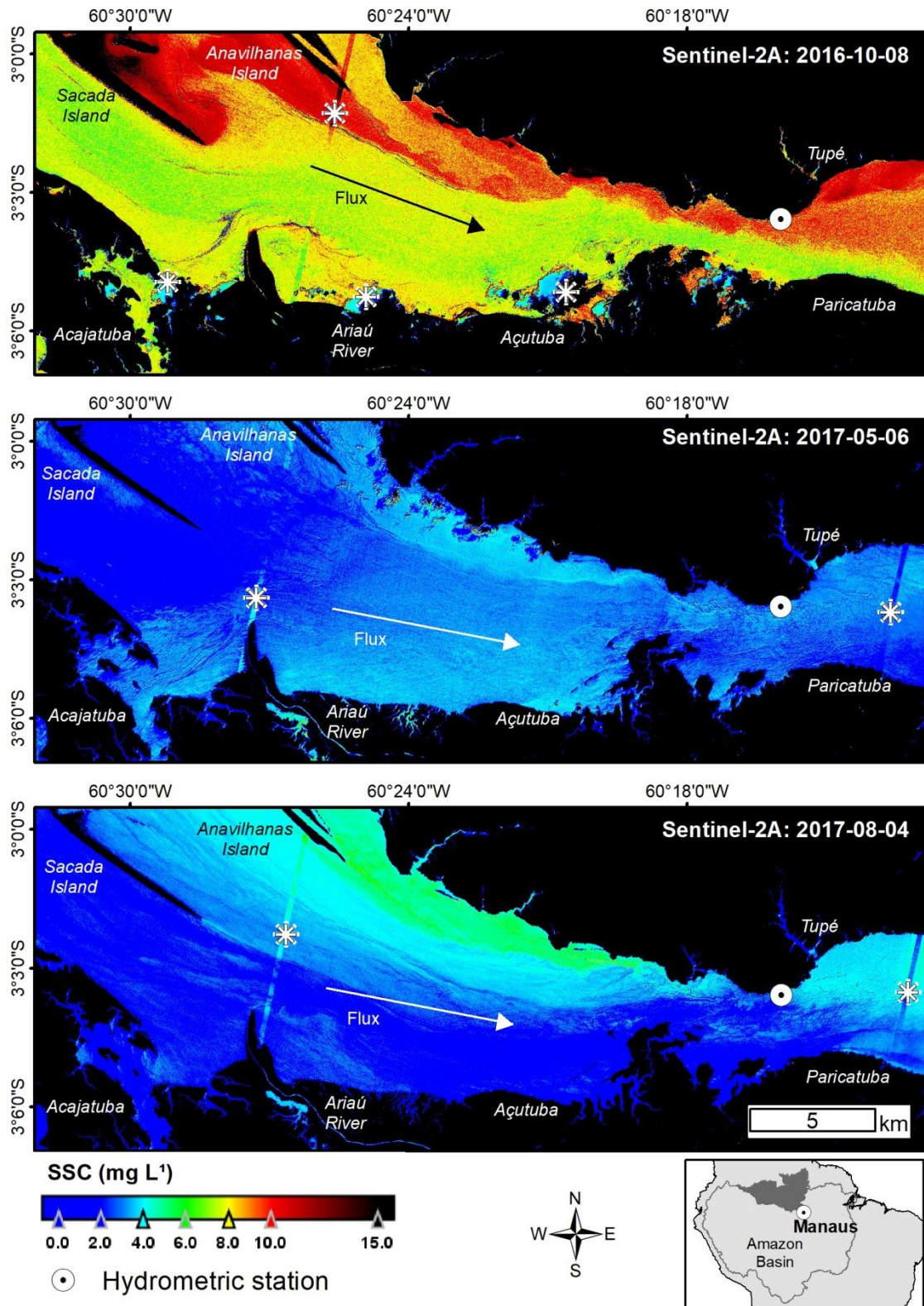


Figure 5. SSC map of the Negro River downstream of Anavilhanas Archipelago estimated with Sentinel-2 images at low (Oct. 2016), high (May 2017), and falling (August 2017) water periods. * Artifact results from sensor calibration.

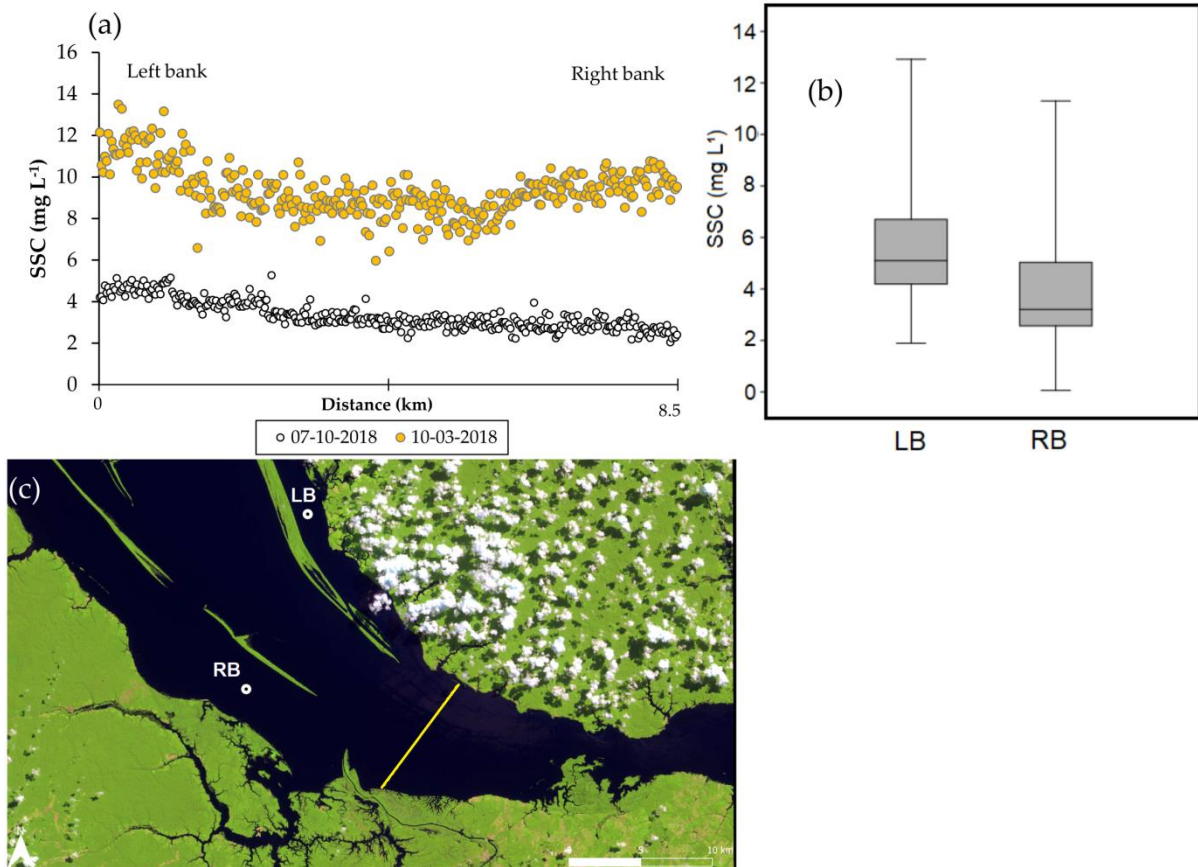


Figure 6. (a) Cross-sectional profile of the SSC over the Negro River estimated using Sentinel-2 images of the high (June 10) and low (October 3) water periods of 2018. (b) Box plot of estimated SSC for the left bank (LB) and right bank (RB) of the Negro River downstream of the Anavilhanas Archipelago. (c) Image with location of LB and RB sections (points) and cross-sectional profile (line).

An example of the combined use of the Sentinel-2A and Sentinel-2B satellites is presented in Figure 7a where we can readily see the spatial and temporal dynamics of suspended sediment in the Paricatuba Strait over 35 days of the Negro River falling water period between July and August 2017. From July 25th to August 4th of 2017, during the transition from high to falling, the suspended sediment presented a higher concentration in the region between the end of Anavilhanas Island and the left bank, while from the second half of August 2017, there was a gradual increase of SSC towards the central region of the channel.

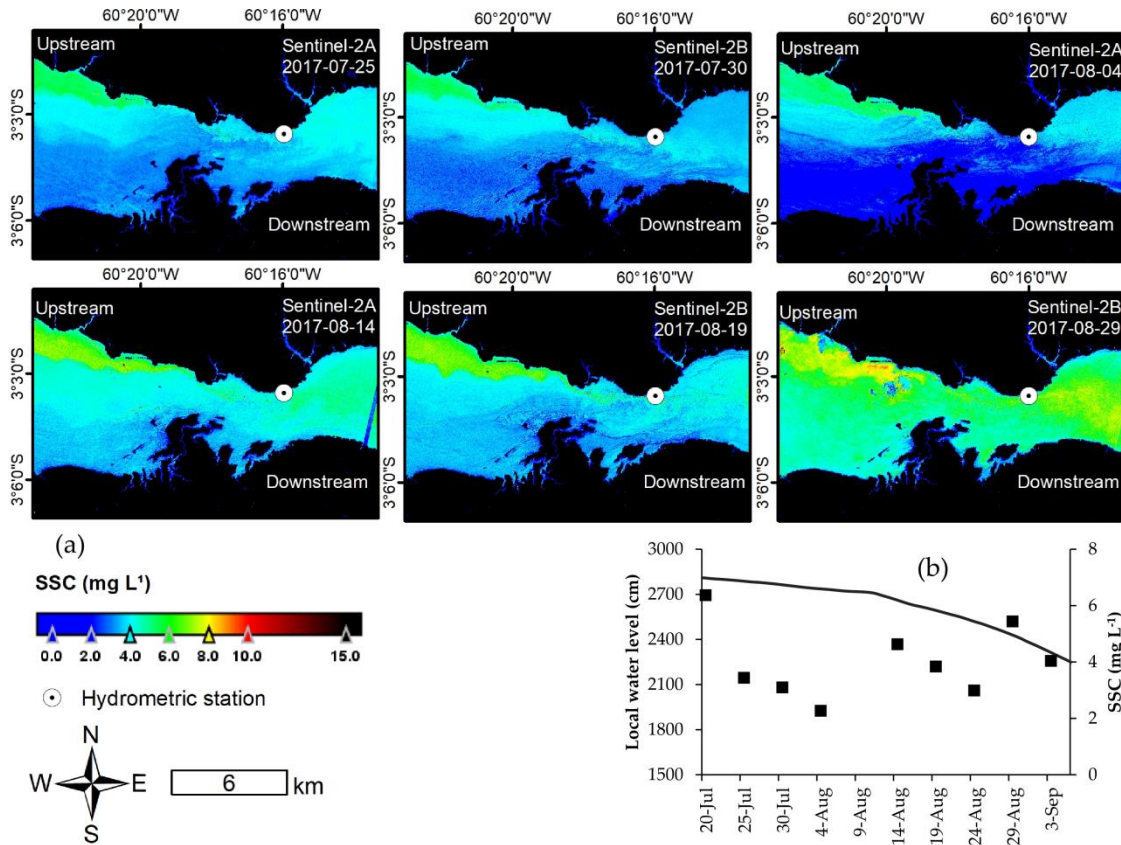


Figure 7. (a) Spatial variation of the SSC of Negro River upstream of Manaus between July 25 and August 29, 2017. (b) Negro River water level (line) and mean SSC (points) of the channel center at the Tatu-Paricatuba hydrometric station between July 20 and September 3, 2017.

In these 35 days of period of falling water levels in the Negro River, the data presented in Figure 7b, derived from the Sentinel-2A and Sentinel-2B satellites, show that the increase in SSC did not occur steadily, but in biweekly pulses, with estimated values of 3.44 mg L⁻¹ on July 25 and 4.63 mg L⁻¹ on August 14 and reaching 5.44 mg L⁻¹ on August 29, 2017.

3.3. The suspended sediment production of the Negro River basin

The monthly variability of the suspended sediment discharge of the Negro River at Manaus, based on the SSC data derived from Sentinel-2, is presented in Figure 8. The estimated monthly mean of sediment discharge varied from 10,571 ton-day⁻¹ for April to 20,771 ton-day⁻¹ for September. Thus, despite the short dataset analyzed in this study (2015–2019), it was observed that sediment fluxes calculated at the Manaus location exhibited a maximum values two months after the water discharge peak.

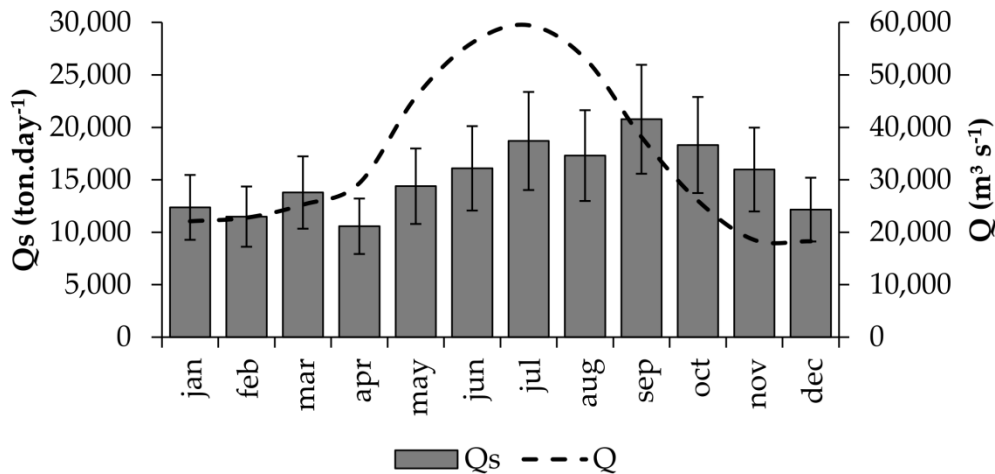


Figure 8. Mean monthly suspended sediment discharge (Qs) and water discharge (Q) regime of the Negro River at Manaus estimated based on mean SSC derived from Sentinel-2 imagery (2015–2019). Vertical lines indicate the standard deviation.

The mean annual water discharge for the analyzed period was 34,573 m³ s⁻¹, and considering the mean SSC of 5.28 mg L⁻¹, a mean annual sediment discharge of the Negro River of 5.76×10⁶ ton·year⁻¹ is estimated, with specific sediment yield (Qsp) in this basin of 8.09 ton·km⁻²·year⁻¹.

4. Discussion

The mean SSC of the lower Negro River estimated with Sentinel-2 images was 40% higher than that observed between 2016-2019 by Marinho, Filizola and Cremon (2020) but close to the values presented in the studies of Meade et al. (1979), Filizola (2003), Moreira-Turcq et al. (2003), and Fassoni-Andrade and Paiva (2019). The results of this study suggest that there might be an inverse relationship between the mean SSC of the Negro River and the precipitation and water level data (Figure 4). Pearson's coefficient showed a negative linear relationship between monthly mean SSC and the river and rainfall regimes, a different dynamic than expected for river systems. However, Marinho, Filizola and Cremon (2020) also observed a negative linear relationship between SSC and the water level of the Negro River in the central region of the Anavilhanas Archipelago.

The suspended sediment transport regime of the Negro River, with a higher concentration in the low water period, is different from the white waters of the other Amazonian rivers, where the maximum suspended load is observed near the flood peak. The Madeira River near its mouth, for example, shows higher SSC one or two months before the flood peak (ESPINOZA-VILLAR et al., 2013). The Purus River near its mouth presents an average SSC of 49 mg L⁻¹ and has peak of SSC in January (of the order of 300 mg L⁻¹); four months before the maximum water discharge (SANTOS et al., 2018). Marinho (2019) analyzed the temporal dynamics of SSC with MODIS sensor data over the lower Negro River over the period 2006–2017 and identified the same pattern observed in the Sentinel-2 data of this study, with the peak of Qs occurring after the peak of Q.

This lag observed between the peak of SSC and peak of flood peak of the Negro River can be understood as a result of the hydraulic control caused by the Amazon River in the region (MEADE et al., 1991) in conjunction with the flood peak of the Branco River at the beginning of the second semester, period of the more outstanding contribution of suspended sediment in the study area (Figure 4b). Between December and March, the Branco River is in the low water period and presents clear waters (CAMPOS, 2011), without much contribution of suspended sediment to the Negro River.

Despite being located in an area of humid tropical climate, the Guiana Shield presents characteristics that do not favor the production of sediments. Of Precambrian age, this shield is composed mainly of crystalline rocks and has little tectonic activity, low to moderate elevation, and sandy soils with a low erosion rate (FILIZOLA and GUYOT, 2009; LATRUBESSE and FRANZINELLI, 2005; LATRUBESSE; STEVAUX; SINHA, 2005). In the Negro River basin, dense forest cover is predominant with a significant part of well-preserved areas due to the low population density, little access by roads, and dangerous navigation (reaches with waterfalls), factors that contribute to low sediment production. The Branco River basin, alternatively, whose drainage area occupies

one-third of the Negro basin, has greater erosion processes due to road accesses and larger deforested areas, in addition to vast areas of less dense forest cover (savannah) in the western region of the basin (CAMPOS, 2011) and a different fluvial regime to that of the Negro River.

Figure 9a shows that there can be a counterclockwise hysteresis of the $SSC = aQ^b$ relationship, in which an inverse exponential relationship can be observed. This peculiar behavior of suspended discharge reduction with increasing water discharge shows a complex system, with a low magnitude in the CSS variation in a large multichannel river with archipelagos, under the influence of the backwater effect of the Amazon River and suspended sediment from the Branco River. However, Marinho, Filizola and Cremon (2020), when analyzing data from 2017 and 2019 (n = 13), did not observe a clear trend in the $SSC = aQ^b$ relationship in Negro River upstream of Anavilhanas. Sander et al. (2015) indicate that the SSC data present high dispersion when related to the water discharge of the Branco River in its middle and upper course, also not showing a clear relationship.

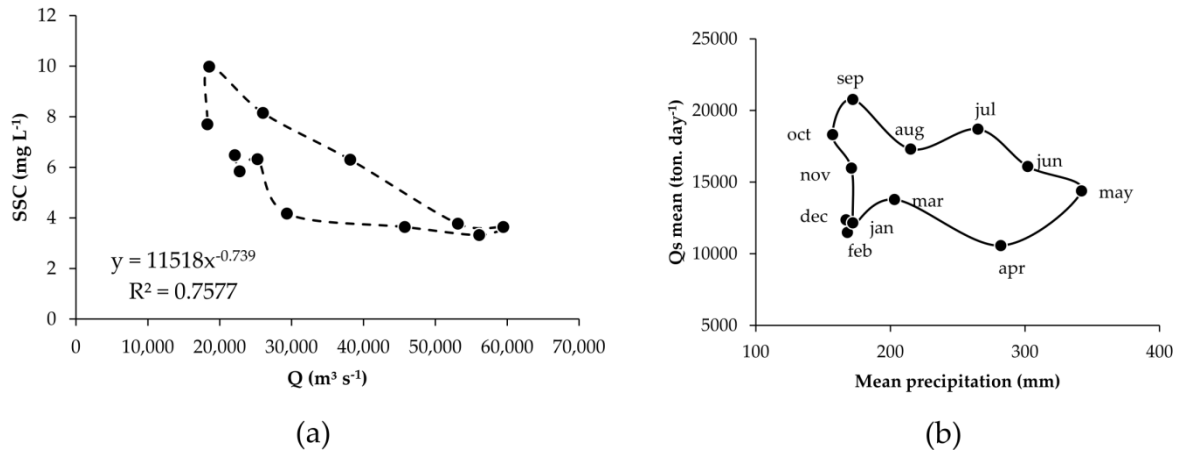


Figure 9. (a) Relation between suspended sediment concentration (SSC) and monthly average water discharge (Q) for Negro River. (b) Relation between suspended sediment discharge (Qs) and monthly average precipitation for Negro River.

Armijos et al. (2020) observed that the discharge of fine suspended sediment (clay and silt) in several Amazonian rivers is controlled by the precipitation regime, while the discharge of coarse sediment (sand) is more related to the variability of the water discharge itself. The suspended sediment transported by the Negro River is composed mainly of particles with a medium silt size, with D50 of 0.25 μm (MARINHO; FILIZOLA; CREMON, 2020), and interestingly, an inverse exponential relationship was observed between SSC and mean monthly precipitation (Figure 4a), but without a clear relationship between Qs and Negro River precipitation, due to the observed hysteresis loop (Figure 9b).

The rise of SSC of the Negro River during the low water period is similar to that observed in lakes connected to the Solimões-Amazonas River plain (BARBOSA et al., 2010; FASSONI-ANDRADE and PAIVA, 2019). For example, Fassoni-Andrade and Paiva (2019) analyzed a set of lakes of the Solimões-Amazonas River plain and detected increased reflectance of the red and near-infrared bands of the MODIS sensor with the reduction of the water level between July and November corresponding to the high and low water periods, respectively. However, some local factors may hinder SSC estimation in these fluvial systems, such as high chlorophyll-a concentration (NOVO et al., 2006) and the background signal in shallow waters (<2 m). With average chlorophyll-a concentration of around 1 $\mu\text{g L}^{-1}$, the Negro River presents a low phytoplankton primary production due to the high concentration of dissolved organic carbon (SCOFIELD et al., 2016).

The temporal variability of the SSC of the Negro River identified in the present study presented the same pattern as that of the Coari and Manacapuru lakes, connected to the Solimões River, evaluated in the study by Fassoni-Andrade and Paiva (2019) with the red band of the MODIS sensor. In these lakes, black waters predominate due to high dissolved organic matter load and low SSC, but the reflectance intensity detected by the MODIS sensor was up to five times higher than that observed by the MSI/Sentinel-2 sensor in the Negro River. These differences may be the results of the methodology used in the atmospheric correction, lack of sunglint correction, and the period of data considered in each study.

The spatial variation of SSC observed in Figure 5, Figure 6, and Figure 7, with higher values at the left margin of the Negro River, is related to the preferential pathway that the suspended sediment has along the left margin

channel of the Anavilhanas Archipelago (MARINHO; FILIZOLA; CREMON, 2020; MARINHO et al., 2021). Thus, factors such as the Branco River with its mouth on the left bank of the Negro River and the structural control on the right bank of the lower Negro River (FRANZINELLI and IGREJA, 2002) contribute to the spatial dynamics of suspended load observed in this region, which in turn causes differences in soil fertility and vegetation type of the islands of Anavilhanas located near the left bank (JUNK et al., 2015; SCABIN; COSTA; SCHÖNGART, 2012).

The broader reaches of the Negro River downstream of Anavilhanas Archipelago was denominated by Latrubesse and Franzinelli (2005) as a dead water area with a possible low hydrosedimentary dynamics in this region. It was observed in Figure 5 that in the dead water area (between the Sacada and Anavilhanas islands), there is a predominance of higher SSC in the image acquired in October 2016, which may indicate a deposition zone of sediment from the Branco River and, owing to its higher concentration concerning the surrounding area, a possible biodiversity hotspot in Anavilhanas. Although the Negro River basin presents the smallest number of hydropower dam in operation in the Amazon, the construction project of the Bem Querer hydropower dam on the Branco River, in Caracaraí city, may result in large ecological impacts to the lower Negro River, mainly owing to the reduction of sediment input and regulation of the hydrological regime (ASSAHIRA et al., 2017; FORSBERG et al., 2017; LATRUBESSE et al., 2017).

Despite the limitations related to the dataset and the temporal interval analyzed, it was observed that the sediment discharge regime (Q_s) of the Negro River with a maximum in the second semester is opposite to the regime of Q_s of the Solimões River at the hydrometric station of Manacapuru (located 109 km upstream of the confluence with the Negro River), of the Amazon River at Óbidos, and of the Madeira River near its mouth, in which the peak of suspended sediment transport occurs typically in the first semester of the year (FILIZOLA and GUYOT, 2009). The sediment production of the basin, of the order of $8 \text{ ton}\cdot\text{km}^{-2}\cdot\text{year}^{-1}$ can be considered the smallest in comparison to the that of great tropical rivers of the world (LATRUBESSE; STEVAUX; SINHA, 2005).

Near the mouth of the Negro River, we estimated an average annual sediment flux of 5.76 million tons per year transported to the Amazon River, a value 25% lower than that presented by Filizola and Guyot (2009) and which represents 1% of the average annual flux of the Amazon River at Óbidos. The sediment production of the Negro River basin, less than $10 \text{ ton}\cdot\text{km}^{-2}\cdot\text{year}^{-1}$, is very low compared to the high precipitation rate of the basin ($>2000 \text{ mm}\cdot\text{year}^{-1}$). Because it drains ancient lands of the Guiana Shield (LATRUBESSE and FRANZINELLI, 2005), this precipitation does not favor the production of suspended sediment. Thus, the low production of sediment in the basin reflects its geological and geomorphological configuration and the result of retention processes of more than 50% of the suspended sediment concerning that which arrives at the Anavilhanas Archipelago (MARINHO; FILIZOLA; CREMON, 2020).

5. Conclusions

This study used Sentinel-2 satellite data to evaluate the suspended sediment transport of the Negro River near its mouth and sediment production in the basin. It was demonstrated that band 4 images from the MSI/Sentinel-2 sensor could be used both to monitor SSC and to study the fluvial geomorphology of the Negro River. The mean SSC estimated was 5.28 mg L^{-1} , varying according to the hydrological period from 3.47 mg L^{-1} during the rising to 8.70 mg L^{-1} during the low water period.

A lag of four months between the peak of water discharge (July) and the peak SSC (November) was detected, different from the pattern of other rivers in the Amazon with white and clear-waters, where the peak of suspended load precedes the flood peak. A strong relationship was observed between the mean monthly variability of SSC and the fluvial regime, with a tendency of increasing suspended load with the reduction of the Negro River water level, which can be related as a response to the joint influence of the Amazon River backwater effect and the hydrosedimentary regime of the Branco River, in lag with the Negro River regime.

Image analysis indicated that part of the suspended sediment from the Branco River, the main tributary of the basin, is retained downstream of the islands of the Anavilhanas Archipelago, suggesting an area of active deposition, which is a different behavior from the idea of a dead water zone as suggested in previous studies. The hydrosedimentary dynamics of the Negro River described in this work suggests that the Guiana Shield provides a suspended sediment flux of the order of 6 million tons per year, an imperceptible contribution concerning the total sediment discharge of the Amazon River near its mouth. The geology and dense forest cover are the main factors contributing to the basin's low sediment production.

Despite the low reflected energy from the Negro River, images from the MSI sensor onboard the Sentinel-2A and Sentinel-2B satellites are sensitive to the low SSC that occurs near Manaus. The Sentinel-2 revisit time of five days limits the use of images in this study area between February and April due to the high cloud cover in the region.

The data presented in this study, together with new acquisitions of the Sentinel-2 constellation, can serve as a reference in future research on the impacts of climate and anthropic activities in the basin on the hydrosediment dynamics downstream Anavilhanas Archipelago. The issue of deforestation and the shift in suspended sediment input from the Branco River as a result of its dam for the Bem Querer Hydroelectric dam stand out in this regard. Finally, we emphasize that the lag observed between the peak SSC and the peak water discharge should be better studied in the future, especially with data observed in situ, which would allow progress in understanding this peculiar hydrosystem.

Supplementary Materials: A Portuguese version of this paper is available online at https://drive.google.com/file/d/1uf9phC_oCi0BqBvhGuXCvYOEbLatI7y/view?usp=sharing

Author Contributions: Conceptualization, RRM, NPF, J-MM and TH; methodology, RRM, NPF and TH; formal analysis, RRM, NPF, J-MM and TH; investigation RRM, NPF and J-MM; resources, NPF and J-MM; data curation, RRM and TH; writing—original draft preparation, RRM and NPF; writing—review and editing, RRM, NPF, J-MM and TH; supervision, NPF and J-MM; funding acquisition, NPF and J-MM. All authors have read and agreed to the published version of the manuscript.

Funding: This research was funded by Universidade Federal do Amazonas [0621/2017]; Institut de Recherche pour le Développement [grant number 262185]; Coordenação de Aperfeiçoamento de Pessoal de Nível Superior—Brasil (CAPES) [1] - the National Academic Cooperation Program in the Amazon (PROCAD/Amazônia Rio Negro TAR Project No. 1709/2018) and The Programme National de Télédétection Spatiale [grant number PNTS-2019-13]. This study was partly funded by CNES through the TOSCA program (project OBS2CO).

Acknowledgments: The first author would like to thank Universidade Federal do Amazonas by the license granted. The authors thank the management team of the Anavilhanas National Park in Novo Airão (ICMBio), the SO-HYBAM Observatory and the two anonymous reviewers who provided valuable suggestions to improve the manuscript.

Conflicts of Interest: The authors declare no conflict of interest. The funders had no role in the design of the study; in the collection, analyses, or interpretation of data; in the writing of the manuscript, or in the decision to publish the results.

References

1. ARMIJOS, E.; CRAVE, A.; ESPINOZA, J. C.; FILIZOLA, N.; ESPINOZA-VILLAR, R.; AYES, I.; FONSECA, P.; FRAIZY, P.; GUTIERREZ, O.; VAUCHEL, P.; CAMENEN, B.; MARTINEZ, J-M.; SANTOS, A.; SANTINI, W.; COCHONNEAU, G.; GUYOT, J-L. Rainfall control on Amazon sediment flux: synthesis from 20 years of monitoring. **Environmental Research Communications**, v. 2, n. 5, p. 051008, 2020. <https://doi.org/10.1088/2515-7620/ab9003>
2. ASSAHIRA, C.; PIEDADE, M.T.F.; TRUMBORE, S.E.; WITTMANN, F.; CINTRA, B.B.L.; BATISTA, E.S.; RESENDE, A.F. DE; SCHÖNGART, J. Tree mortality of a flood-adapted species in response of hydrographic changes caused by an Amazonian river dam. **For. Ecol. Manage**, v. 396, p. 113-123, 2017. <https://doi.org/10.1016/j.foreco.2017.04.016>
3. BARBOSA, C. C. F.; NOVO, E. M. L.; MELACK, J. M.; GASTIL-BUHL, M.; FILHO, W. P.. Geospatial analysis of spatiotemporal patterns of pH, total suspended sediment and chlorophyll-a on the Amazon floodplain. **Limnology**, v. 11, n. 2, p. 155-166, 2010. <https://doi.org/10.1007/s10201-009-0305-5>
4. BUKATA, R. P. **Satellite monitoring of inland and coastal water quality: retrospection, intropection, future direction**. Boca Raton: Taylor and Francis, 2005. 272p.
5. CAMPOS, C. **Diversidade socioambiental de Roraima: subsídios para debater o futuro Sustentável da Região**. São Paulo: Socioenvironmental Institute, 2011. 35p.
6. CHARLTON, R. **Fundamentals of Fluvial Geomorphology**. London : Routledge, 2007. 280p.
7. CHIRPS. **The CHIRPS dataset website, 2015**. Available at: <<https://www.chc.ucsb.edu/data/chirps>>. Accessed 17 May 2018
8. COSTA, J. C.; PEREIRA, G.; SIQUEIRA, M. E.; DA SILVA CARDOZO, F.; DA SILVA, V. V. Validation of precipitation data estimated by CHIRPS for Brazil. **Revista Brasileira de Climatologia**, v. 24, p. 228-243, 2019.
9. DOXARAN, D.; FROIDEFOND, J-M.; LAVENDER, S.; CASTAING, P. Spectral signature of highly turbid waters. **Remote Sensing of Environment**, v. 81 n. 1, p. 149-161, 2002. [https://doi.org/10.1016/S0034-4257\(01\)00341-8](https://doi.org/10.1016/S0034-4257(01)00341-8)
10. DRUSCH, M.; DEL BELLO, U.; CARLIER, S.; COLIN, O.; FERNANDEZ, V.; GASCON, F.; HOERSCH, B.; ISOLA, C.; LABERINTI, P.; MARTIMORT, P.; MEYGRET, A.; SPOTO, F.; SY, O.; MARCHESE, F.; BARGELLINI, P. Sentinel-2: ESA's

- Optical High-Resolution Mission for GMES Operational Services. **Remote Sensing of Environment**, v. 120, p. 25-36, 2012. <https://doi.org/10.1016/j.rse.2011.11.026>
11. ESPINOZA-VILLAR, R.; MARTINEZ, J-M.; ARMIJOS, E.; ESPINOZA, J-C.; FILIZOLA, N.; SANTOS, A.; WILLEMS, B.; FRAIZY, P.; SANTINI, W. ; VAUCHEL, P. Spatio-temporal monitoring of suspended sediments in the Solimões River (2000-2014). **Comptes Rendus Geoscience**, v. 350 n. 1-2, p. 4-12, 2018. <https://doi.org/10.1016/j.crte.2017.05.001>
 12. ESPINOZA-VILLAR, R.; MARTINEZ, J-M.; LE TEXIER, M.; GUYOT, J-L.; FRAIZY, P.; MENESES, P. ; OLIVEIRA, E. A study of sediment transport in the Madeira River, Brazil, using MODIS remote-sensing images. **Journal of South American Earth Sciences**, v. 44, p. 45-54. 2013. <https://doi.org/10.1016/j.jsames.2012.11.006>
 13. FASSONI-ANDRADE, A. C.; PAIVA, R. C. D. Mapping spatial-temporal sediment dynamics of river-floodplains in the Amazon. **Remote Sensing of Environment**, v. 221, p. 94-107, 2019. <https://doi.org/10.1016/j.rse.2018.10.038>
 14. FILIZOLA, N. P. **O fluxo de sedimentos em suspensão nos rios da Amazônia Brasileira**. Brasília: ANEEL, 1999. 63p.
 15. FILIZOLA, N. P. **Transfert sédimentaire actuel par les fleuves amazoniens**. Thesis (Doctorate in Geology) - Graduate Program in Geology, Université Toulouse III - Paul Sabatier. 2003. 283p.
 16. FILIZOLA, N.; GUYOT, J-L.; WITTMANN, H.; MARTINEZ, J-M.; OLIVEIRA, E. The Significance of Suspended Sediment Transport Determination on the Amazonian Hydrological Scenario. In: MANNING, A. J. (ed). **Sediment Transport in Aquatic Environments**. Rijeka: InTech, 2011. p. 45-64. <https://doi.org/10.5772/19948>
 17. FILIZOLA, N. ; GUYOT, J-L. Suspended sediment yields in the Amazon basin: an assessment using the Brazilian national data set. **Hydrological Processes**, v. 23, n. 22, p. 3207-3215, 2009. <https://doi.org/10.1002/hyp.7394>
 18. FILIZOLA, N. ; GUYOT, J-L. Fluxo de sedimentos em suspensão nos rios da Amazônia. **Revista Brasileira de Geociências**, v. 41, n. 4, p. 566-576, 2011. <https://doi.org/10.25249/0375-7536.2011414566576>
 19. FILIZOLA, N.; SEYLER, F.; MOURÃO, H.; ARRUDA, W.; SPINOLA, N.; GUYOT, J-L. Study of the variability in suspended sediment discharge at Manacapuru, Amazon River, Brazil. **Latin American Journal of Sedimentology and Basin Analysis**, v. 16, p. 93-99, 2009.
 20. FORSBERG, B.R.; MELACK, J.M.; DUNNE, T.; BARTHEM, R.B.; GOULDING, M.; PAIVA, R.C.D.; SORRIBAS, M.V.; SILVA, U.L.; WEISSER, S. The potential impact of new Andean dams on Amazon fluvial ecosystems. **PLoS ONE**, v. 12, p. e0182254, 2017. <https://doi.org/10.1371/journal.pone.0182254>
 21. FRANZINELLI, E.; IGREJA, H. Modern sedimentation in the Lower Negro River, Amazonas State, Brazil. **Geomorphology**, v. 44, p. 259-271, 2002. [https://doi.org/10.1016/S0169-555X\(01\)00178-7](https://doi.org/10.1016/S0169-555X(01)00178-7)
 22. GUPTA, A. **Large rivers: geomorphology and management**. Chichester: John Wiley and Sons, 2007. 712p.
 23. HARMEL, T.; CHAMI, M.; TORMOS, T.; REYNAUD, N.; DANIS, P-A. Sunlight correction of the Multi-Spectral Instrument (MSI)-SENTINEL-2 imagery over inland and sea waters from SWIR bands. **Remote Sensing of Environment**, v. 204, p. 308-321, 2018. <https://doi.org/10.1016/j.rse.2017.10.022>
 24. HYBAM. **Observation Service SO HYBAM**. Available at: < <http://www.ore-hybam.org>>. Accessed on: 29 Dec 2018
 25. JUNK, W.J.; WITTMANN, F.; SCHÖNGART, J.; PIEDADE, M.T.F. A classification of the major habitats of Amazonian black-water river floodplains and a comparison with their white-water counterparts. **Wetl. Ecol. Manag.**, vol. 23, p. 677-693, 2015. <https://doi.org/10.1007/s11273-015-9412-8>.
 26. LATRUBESSE, E. M. Patterns of anabranching channels: The ultimate end-member adjustment of mega rivers. **Geomorphology**, v. 101, n. 1-2, p. 130-145, 2008. <https://doi.org/10.1016/j.geomorph.2008.05.035>
 27. LATRUBESSE, E. M. ; FRANZINELLI, E. The late Quaternary evolution of the Negro River, Amazon, Brazil: Implications for island and floodplain formation in large anabranching tropical systems. **Geomorphology**, v. 70, n. 4, p. 372-397, 2005. <https://doi.org/10.1016/j.geomorph.2005.02.014>
 28. LATRUBESSE, E. M.; STEVAUX, J. C. ; SINHA, R. Tropical rivers. **Geomorphology**, v. 70, n. 3-4, p. 187-206, 2005. <https://doi.org/10.1016/j.geomorph.2005.02.005>
 29. LATRUBESSE, E.M.; ARIMA, E.Y.; DUNNE, T.; PARK, E.; BAKER, V.R.; D'HORTA, F.M.; WIGHT, C.; WITTMANN, F.; ZUANON, J.; BAKER, P.A.; et al. Damming the rivers of the Amazon basin. **Nature**, v. 546, p. 363-369, 2017. <https://doi.org/10.1038/nature22333>
 30. LEENHEER, J. A. Origin and nature of humic substances in the waters of the Amazon River Basin. **Acta Amazonica**, v. 10, n. 3, p. 513-526, 1980. <https://doi.org/10.1590/1809-43921980103513>
 31. LI, J.; ROY, D. P. A Global Analysis of Sentinel-2A, Sentinel-2B and Landsat-8 Data Revisit Intervals and Implications for Terrestrial Monitoring. **Remote Sensing**, v. 9, p. 902, 2017. <https://doi.org/10.3390/rs9090902>
 32. MARINHO, R. R. **Integration of field data and remote sensing in the study of water and matter flux in the Anavilhanas Archipelago, Rio Negro - Amazonas, Brazil**. Thesis (PhD in Climate and Environment) - Graduate Program in Climate and Environment, National Institute for Amazon Research, Manaus. 2019.160p.

33. MARINHO, R. R.; FILIZOLA, N. P. ; CREMON, É. H. Analysis of Suspended Sediment in the Anavilhanas Archipelago, Rio Negro, Amazon Basin. **Water**, v. 12, p. 1073, 2020. <https://doi.org/10.3390/w12041073>
34. MARINHO, R.R.; HARMEL, T.; MARTINEZ, J.-M.; FILIZOLA JUNIOR, N.P. Spatiotemporal Dynamics of Suspended Sediments in the Negro River, Amazon Basin, from In Situ and Sentinel-2 Remote Sensing Data. **ISPRS Int. J. Geo-Information**, vol. 10, n. 2, p.86, 2021. <https://doi.org/10.3390/w12041073>
35. MARTINEZ, J.-M.; ESPINOZA-VILLAR, R.; ARMIJOS, E.; MOREIRA, L. The optical properties of river and floodplain waters in the Amazon River Basin: Implications for satellite-based measurements of suspended particulate matter. **Journal of Geophysical Research: Earth Surface**, v. 120, n. 7, p. 1274-1287. 2015. <https://doi.org/10.1002/2014JF003404>
36. MEADE, R. H.; NORDIN, C. F.; CURTIS, W. F.; RODRIGUES, F. M. C.; VALE, C. M. ; EDMOND, J. M. Sediment transport in the Amazon River. **Acta Amazonica**, v. 9, n. 3, p. 543-547, 1979. <https://doi.org/10.1590/1809-43921979093543>
37. MEADE, R.H.; RAYOL, J.M.; CONCEIÇÃO, S.C.; NATIVIDADE, J.R.G. Backwater effects in the Amazon River basin of Brazil. **Environmental Geology and Water Sciences**, v. 18, n. 2, p.105-114, 1991. <https://doi.org/10.1007/BF01704664>
38. MILLIMAN, J. D.; FARNSWORTH, K. **River Discharge to the Coastal Ocean - A Global Synthesis**. Indiana: Indiana University of Pennsylvania, 2011. 394p.
39. MOLINIER, M.; GUYOT, J.-L.; OLIVEIRA, E. ; GUIMARAES, V. Les régimes hydrologiques de l'Amazone et de ses affluents. In: CHEVALLIER, P. ; POUYAUD, B. (eds). **L'hydrologie tropicale: géosciences et outil pour le développement: mélanges à la mémoire de Jean Rodier**. Paris, IAHS, p. 209-222. 1996.
40. MONTANHER, O. C.; NOVO, E. M. L. M.; BARBOSA, C. C. F.; RENNO, C. D.; SILVA, T. S. F. Empirical models for estimating the suspended sediment concentration in Amazonian white water rivers using Landsat 5/TM. **International Journal of Applied Earth Observation and Geoinformation**, v. 29, p. 67-77, 2014. <https://doi.org/10.1016/j.jag.2014.01.001>
41. MORA, A.; LARAQUE, A.; MOREIRA-TURCO, P.; ALFONSO, J.A. Temporal variation and fluxes of dissolved and particulate organic carbon in the Apure, Caura and Orinoco rivers, Venezuela. **J. South Am. Earth Sci.**, v. 54, p.47-56, 2014. <https://doi.org/10.1016/j.jsames.2014.04.010>
42. MOREIRA-TURCO, P.; SEYLER, P.; GUYOT, J.-L. ; ETCHEBER, H. Exportation of organic carbon from the Amazon River and its main tributaries. **Hydrological Processes**, v. 17, n. 7, p. 1329-1344, 2003. <https://doi.org/10.1002/hyp.1287>
43. NOVO, E.M.L. DE M.; BARBOSA, C.C.F.; FREITAS, R.M.; SHIMABUKURO, Y.E.; MELACK, J.M.; FILHO, W.P. Seasonal changes in chlorophyll distributions in Amazon floodplain lakes derived from MODIS images. **Limnology**, v. 7, p.153-161, 2006. <https://doi.org/10.1007/s10201-006-0179-8>
44. RICHEY, J. E.; HEDGES, J. I.; DEVOL, A. H.; QUAY, P. D.; VICTORIA, R.; MARTINELLI, L.; FORSBERG B. R. Biogeochemistry of carbon in the Amazon River. **Limnology and Oceanography**, v. 35, n. 2, p. 352-371, 1990. <https://doi.org/10.4319/lo.1990.35.2.0352>
45. SANDER, C.; GASPARETTO, N. V. L.; SANTOS, M. L.; CARVALHO, T. M. Characteristics of suspended sediment transport in the Rio Branco basin, State of Roraima. **Acta Geográfica**, v. 8, n. 17, p. 71-85, 2014.
46. SANTOS, A. L. M. R.; MARTINEZ, J.-M.; FILIZOLA, N.; ARMIJOS, E.; ALVES, L. G. S. Purus River suspended sediment variability and contributions to the Amazon River from satellite data (2000-2015). **Comptes Rendus Geoscience**, v. 350, n. 1-2, p. 13-19, 2018. <https://doi.org/10.1016/j.crte.2017.05.004>
47. SCABIN, A.B.; COSTA, F.R.C.; SCHÖNGART, J. The spatial distribution of illegal logging in the Anavilhanas archipelago (Central Amazonia) and logging impacts on species. **Environ. Conserv.** v. 39, p. 111-121, 2012. <https://doi.org/10.1017/S0376892911000610>
48. SCOFIELD, V.; MELACK, J.M.; BARBOSA, P.M.; AMARAL, J.H.F.; FORSBERG, B.R.; FARJALLA, V.F. Carbon dioxide outgassing from Amazonian aquatic ecosystems in the Negro River basin. **Biogeochemistry**, v. 129, p. 77-91, 2016. <https://doi.org/10.1007/s10533-016-0220-x>
49. TUCCI, C.E.M. **Hidrologia: Ciência e Aplicação**. Porto Alegre: UFRGS/ABRH, 2012. 944p.
50. WITTMANN, H.; VON BLANCKENBURG, F.; MAURICE, L.; GUYOT, J.-L.; FILIZOLA, N. ; KUBIK, P. W. Sediment production and delivery in the Amazon River basin quantified by in situ-produced cosmogenic nuclides and recent river loads. **Geological Society of America Bulletin**, v. 123, n. 5-6, p. 934-950, 2011. <https://doi.org/10.1130/B30317.1>



Esta obra está licenciada com uma Licença Creative Commons Atribuição 4.0 Internacional (<http://creativecommons.org/licenses/by/4.0/>) – CC BY. Esta licença permite que outros distribuam, remixem, adaptem e criem a partir do seu trabalho, mesmo para fins comerciais, desde que lhe atribuam o devido crédito pela criação original.